Supporting Information for

Functionalisation of MOFs open metal sites with pendant amines for CO_2 capture

Carmen Montoro,[a] Elena García,[b] Sofia Calero,[b] Maria Pérez-Fernández,[c] Antonio L. López,[c] Elisa Barea[a] and Jorge A. R. Navarro[a]

[a]*Departamento de Química Inorgánica, Universidad de Granada, Av. Fuentenueva S/N, 18071 Granada, Spain. Fax: (+34) 958-248526, jarn@ugr.es; http://www.ugr.es/local/jarn*

[b] *Departamento de Sistemas Físicos, Químicos y Naturales*

Universidad Pablo de Olavide

41013 Sevilla, Spain

[c] *R&D Department. CCS Technologies*

INABENSA

CIL Torrecuéllar, Sevilla, Spain

General methods

All the general reagents and solvents were commercially available and used as received. Ethylenediamine (en), 3 – picolylamine (3pico) and 4 – picolylamine (4pico) were purchased from Sigma Aldrich. $[Cu_3(1,3,5\text{-benzenetricarboxylato})_2]$ (**1**)[1] was prepared according to published procedures. Thermogravimetric analyses were performed, using a reactive air atmosphere, on a Shimadzu-TGA-50H equipment, at a heating rate of 20 K min^{-1}. XRPD data were obtained on a D2 PHASER Bruker diffractometer using CuKα radiation (λ = 1.5418 Å). The compounds were manually grounded in an agate mortar and then deposited in the hollow of a zero-background silicon sample holder. Adsorption isotherms were measured at 77 K for N_2 and at 273, 298 and 323 K for CO_2, on a Micromeritics Tristar 3000 volumetric instrument. Prior to measurement, powder samples were heated 7 h (at 453 K for $[Cu_3(btc)_2]$ and at 393 K for the rest of the componds) and outgassed to 10^{-1} Pa.

HKUST grafting with amines

The functionalization of the coordinately unsaturated Cu^{II} sites was accomplished using a procedure analogous to that reported for MIL-101.[2] First of all, **1** was to be activated at 393 K and outgassed to 10^{-1} Pa, to obtain the porous matrix evacuated with free cavities available for the adsorption of other molecules of interest. To a suspension of **1** in toluene, was added the corresponding amine. Best results were obtained for a 1:1 Cu:amine ratio. The resulting suspension was refluxed under N_2 for 12 h to optimize the extent of amine grafting, and the solid product was washed copiously with hexane to ensure complete removal of non-appended substituent.

Anal. calc. for $Cu_3(C_9H_3O_6)_2(C_2H_8N_2)_{2.4}(H_2O)_8$ (**1@en**): C, 30.6; H, 4.65; N, 7.5; Anal. Found: C, 30.47; H, 5.24; N, 7.46. Considering Z = 16, the functionalization degree of 1@en is 38.4 amines for unit cell.

Anal. calc. for $Cu_3(C_9H_3O_6)_2(C_6H_8N_2)_2(H_2O)_4(C_7H_8)_{0.5}$ (**1@3pico**): C, 42.84; H, 3.65; N, 5.96; Anal. Found C, 42.73; H, 3.68; N, 5.76. Considering Z = 16, the functionalization degree of 1@3pico is 32 amines for unit cell.

Anal. calc. for $Cu_3(C_9H_3O_6)_2(C_6H_8N_2)_{1.5}(H_2O)_4(C_7H_8)_{0.8}$ (**1@4pico**): C, 42.89; H, 3.58; N, 4.60; Anal. Found: C, 43.04; H, 3.43; N, 4.36. Considering Z = 16, the functionalization degree of 1@4pico is 24 amines for unit cell.

Powder X-Ray Diffraction

The samples were deposited in the hollow of an aluminum sample holder equipped with a zero-background plate. Diffraction data were collected by means of a scan in the 2θ range of 5-35° with 0.02°, steps using a D2 PHASER Bruker diffractometer using CuKα radiation (λ = 1.5418 Å).

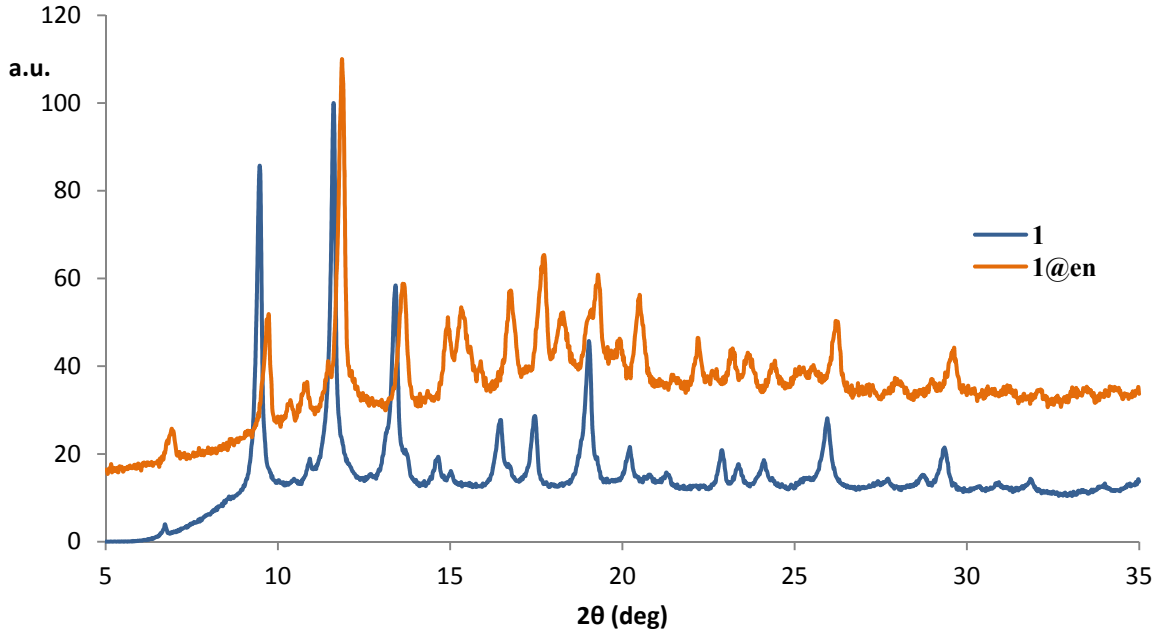

Figure S1. XRPDs for **1** and **1@en**.

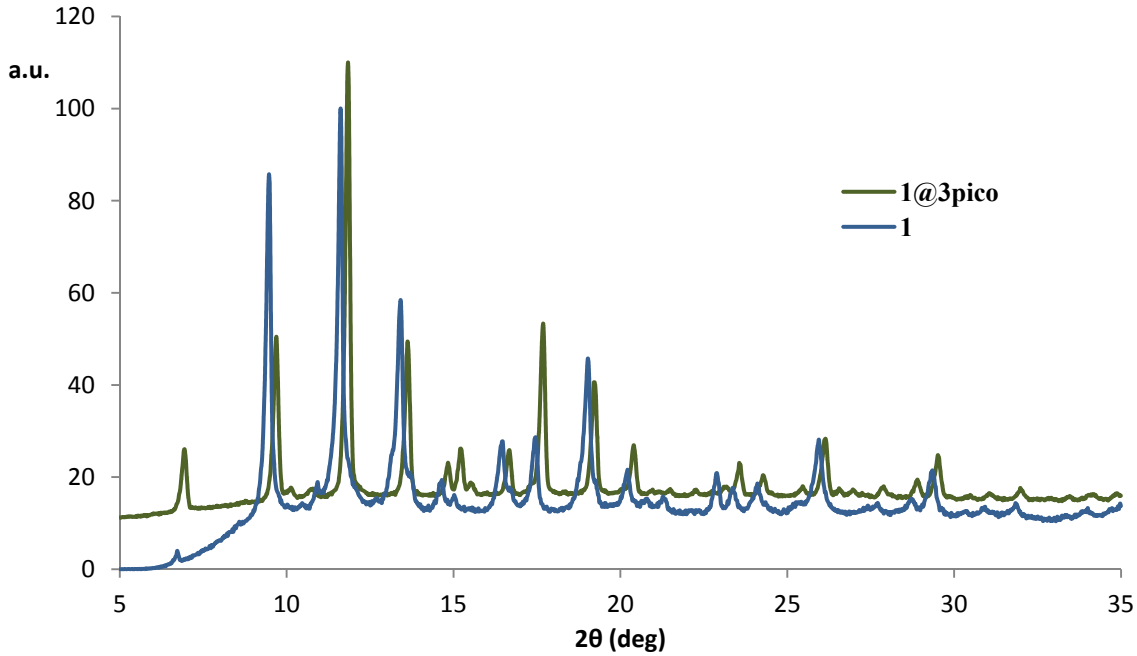

Figure S2. XRPDs for **1** and **1@3pico**.

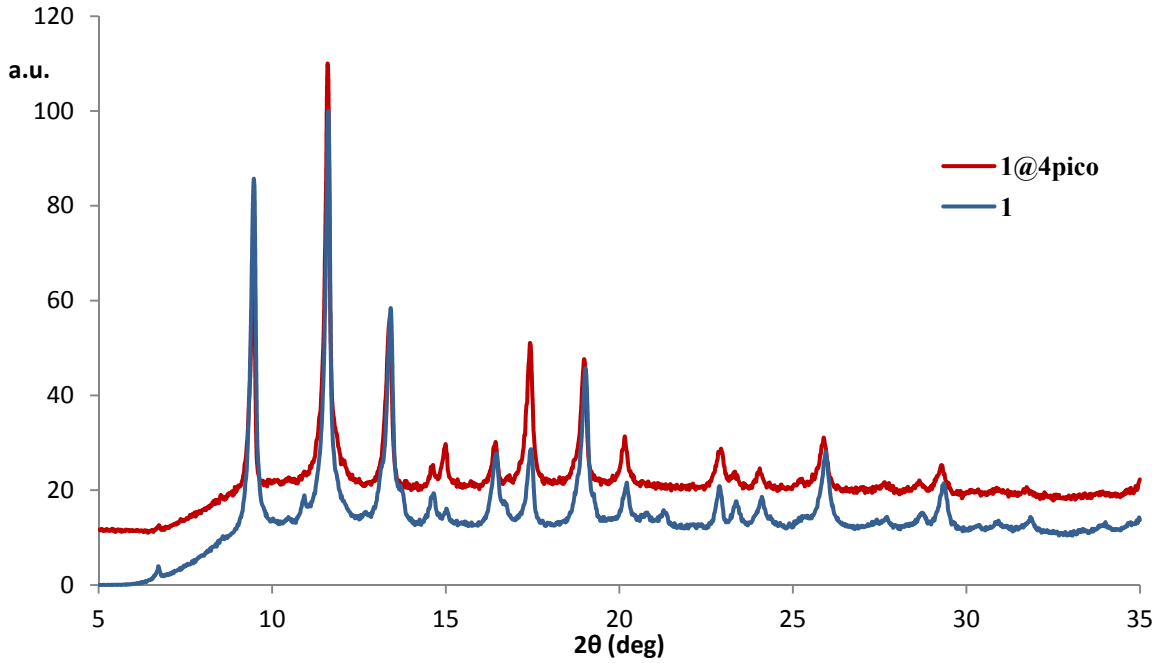

Figure S3. XRPDs for **1** and **1@4pico**.

Thermal Analysis

Thermogravimetry

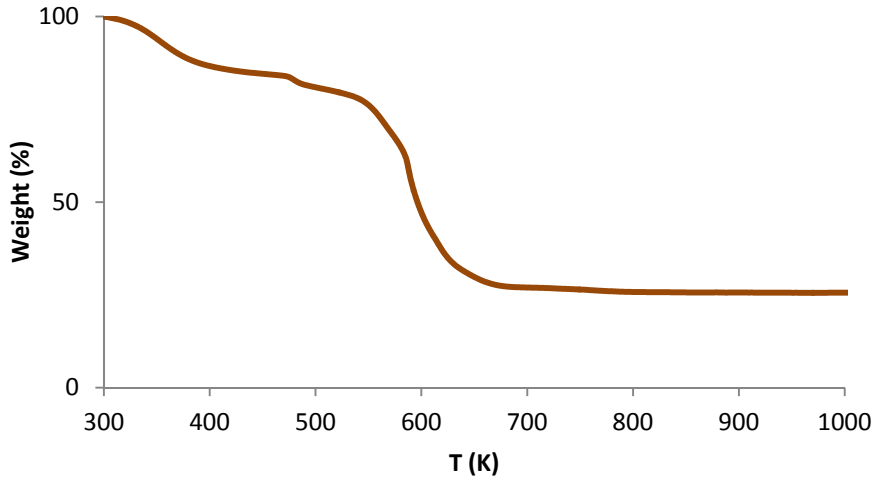

Figure S4. TGA trace for species **1@en**.

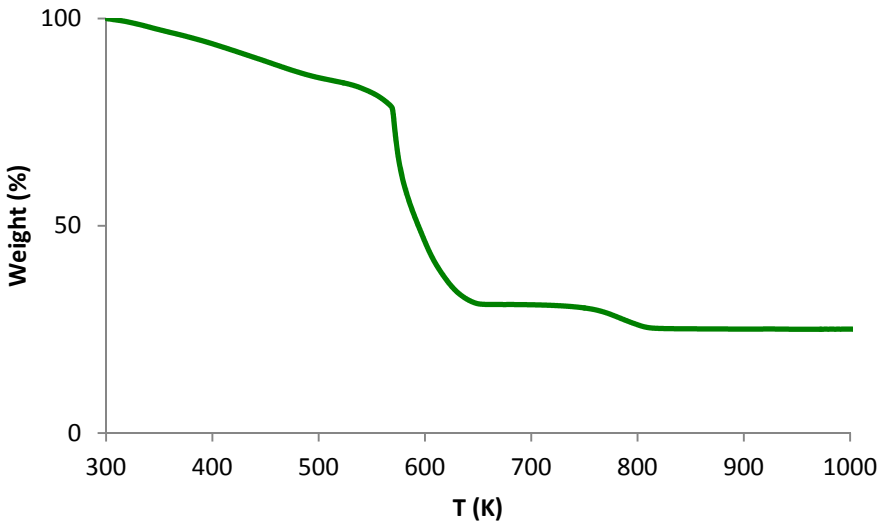

Figure S5. TGA trace for species **1@3pico**.

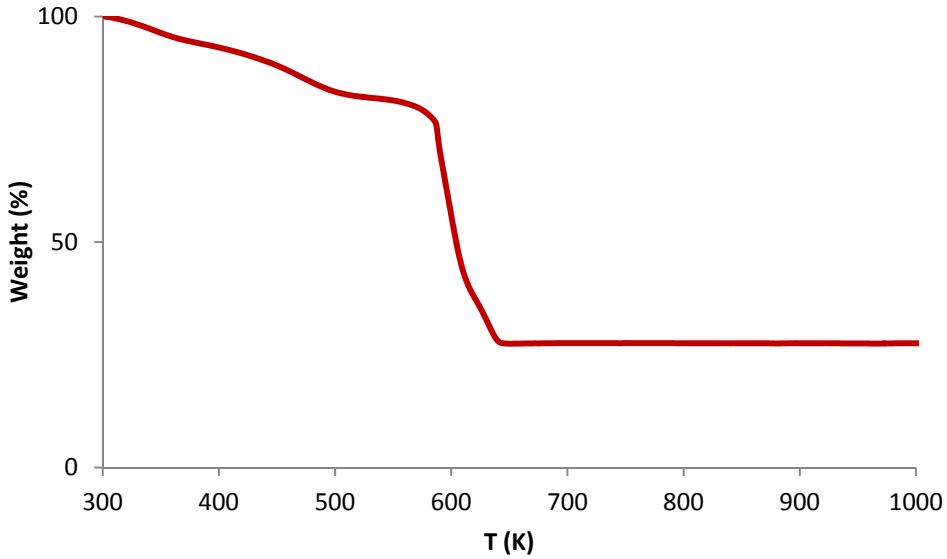

Figure S6. TGA trace for **1@4pico** species.

Gas adsorption measurements

The gas adsorption isotherms were measured on a Micromeritics Tristar 3000 volumetric instrument. Prior to measurement, powder samples were heated 7 h (at 453 K for $[Cu_3(btc)_2]$ and at 393 K for the rest of the componds) and outgassed to 10^{-1} Pa.

N_2 adsorption isotherms

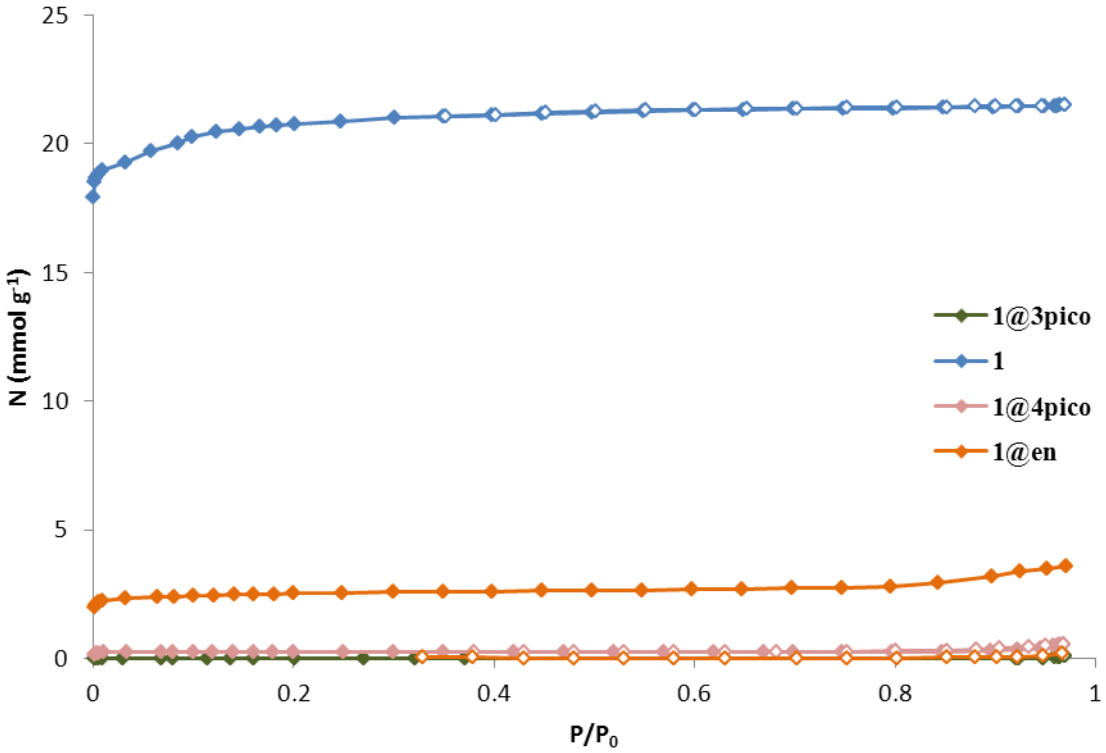

Figure S7. N_2 adsorption isotherms at 77 K for **1**, **1@en**, **1@3pico** and **1@4pico**.

CO_2 adsorption isotherms at 273K

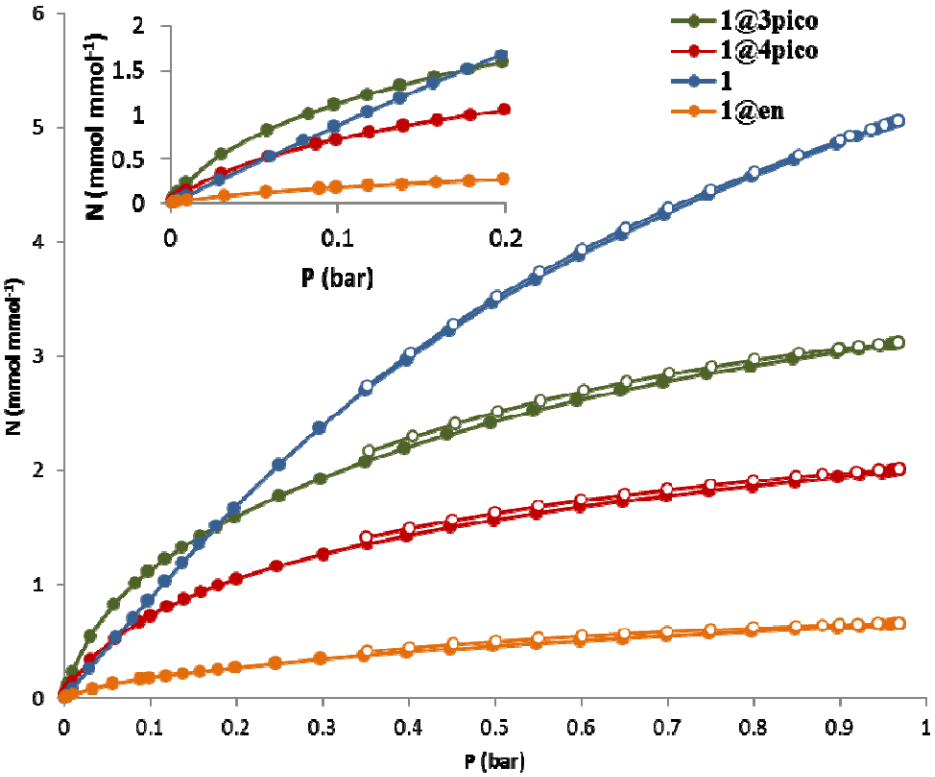

Figure S8. CO_2 adsorption isotherms at 273 K for **1**, **1@en**, **1@3pico** and **1@4pico**.

CO_2 adsorption isotherms at 298K

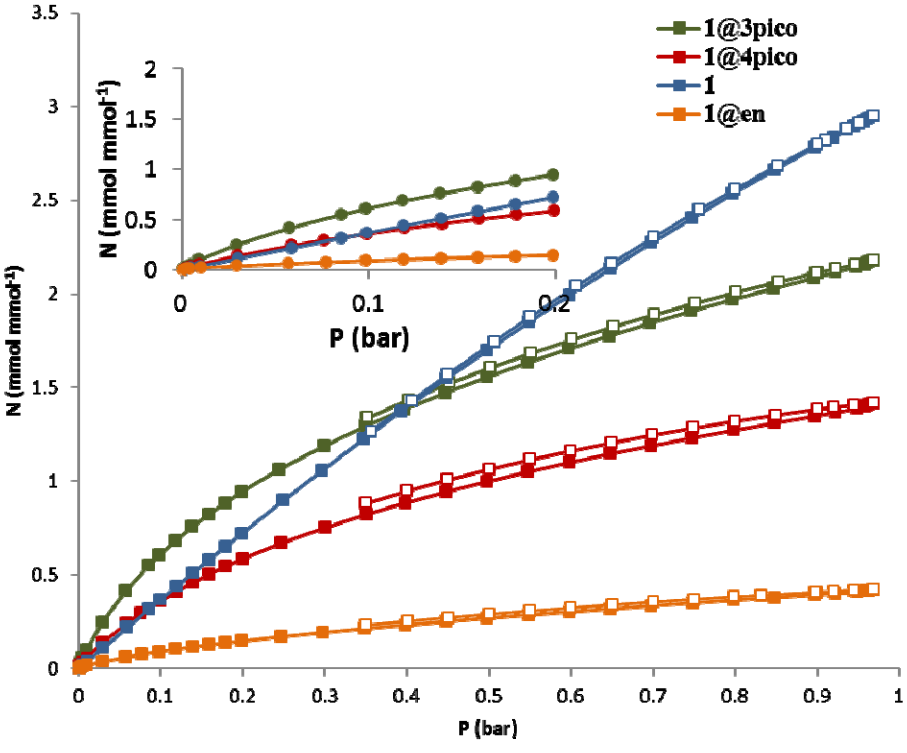

Figure S9. CO_2 adsorption isotherms at 298 K for **1**, **1@en**, **1@3pico** and **1@4pico**.

CO_2 adsorption isotherms at 323K

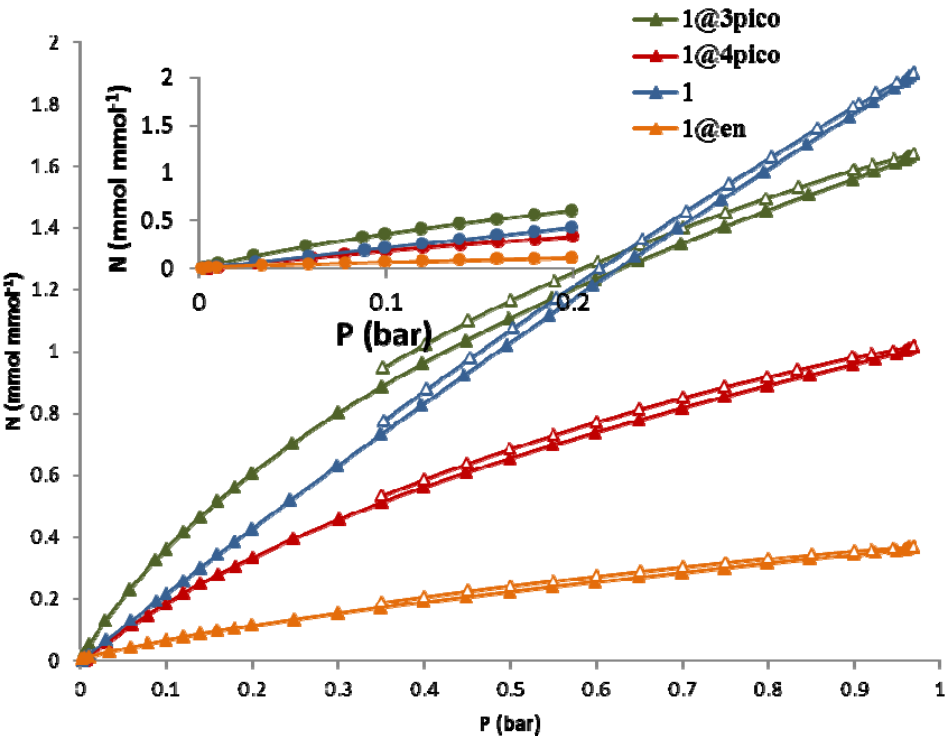

Figure S10. CO_2 adsorption isotherms at 323 K for **1**, **1@en**, **1@3pico** and **1@4pico**.

Mechanical Stress Tests

Mechanical stress tests were performed on **1** and **1@3pico**. A typical test consisted on the characterization, by XRPD and N_2 and CO_2 adsorption isotherms of pellets fabricated, with 100 mg of the original sample and after grounding trough a 0.5 mm sieve, by the application of specific values of pressure, up to 0.2 GPa (2 tonns cm^{-2}) and 0.4 GPa (4 tonns cm^{-2}).

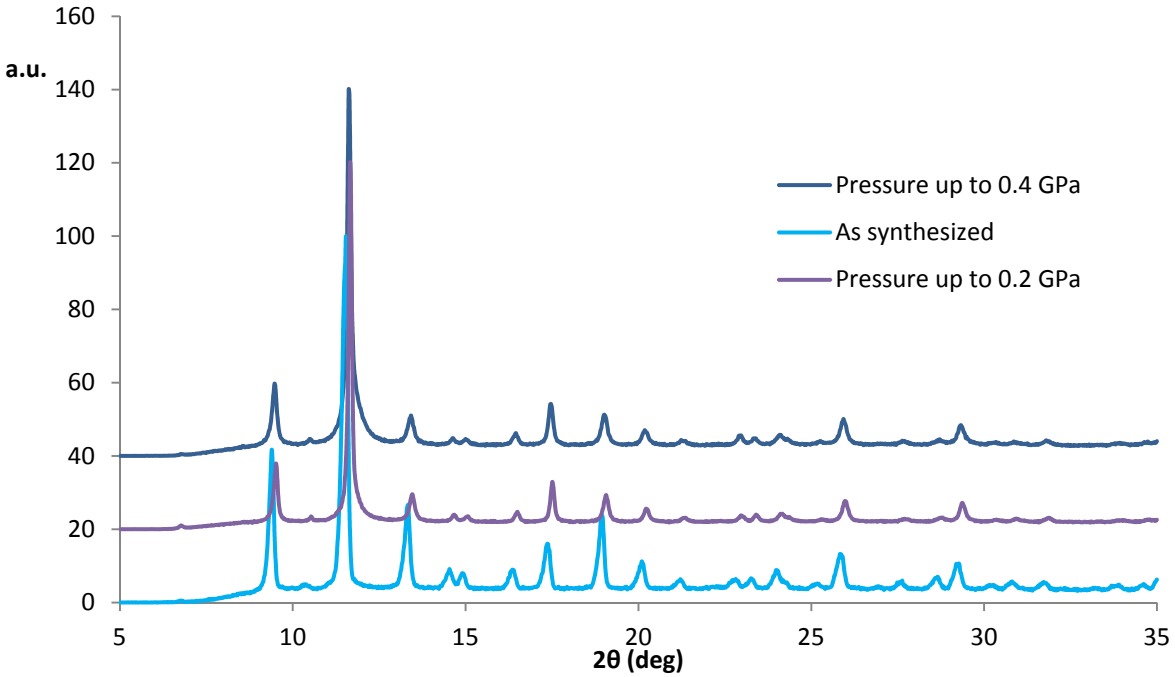

Figure S11. XRPD data for **1** before and after the mechanical stress tests.

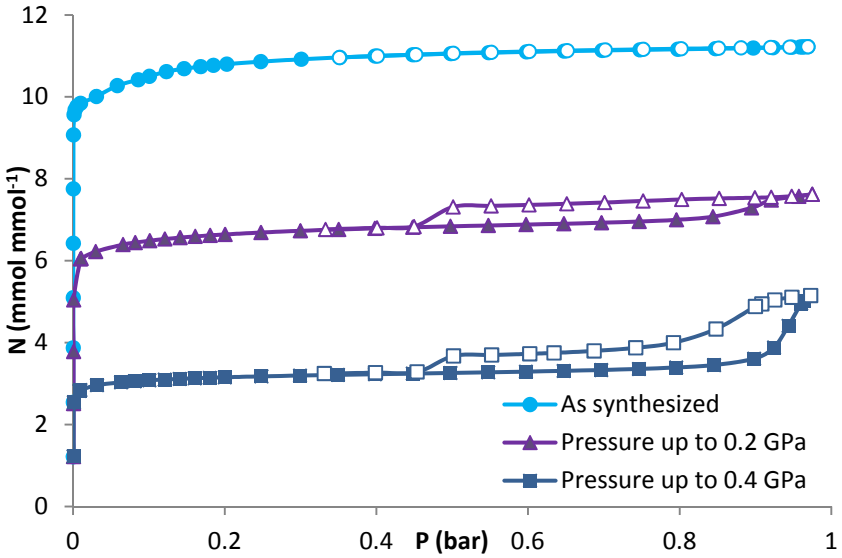

Figure S12. N_2 adsorption isotherms at 77 K for **1** before and after the mechanical stress tests. Desorption branches of the isotherms are depicted with empty symbols.

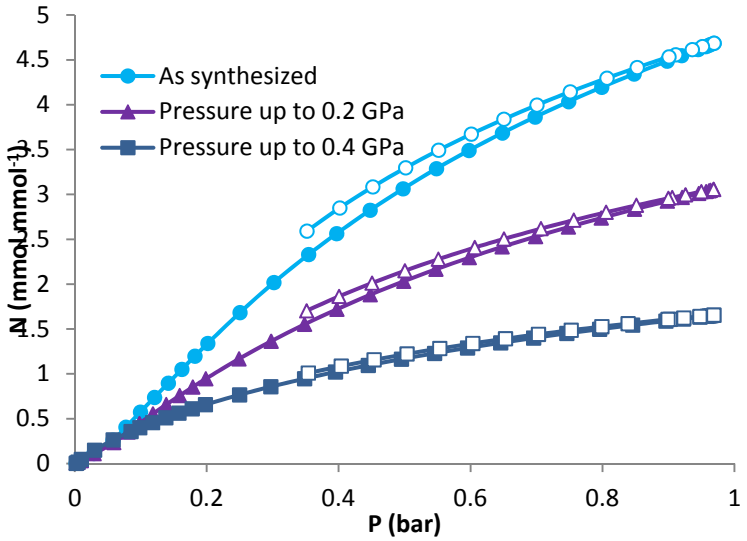

Figure S13. CO_2 adsorption isotherms at 273 K for **1** before and after the mechanical stress tests. Desorption branches of the isotherms are depicted with empty symbols.

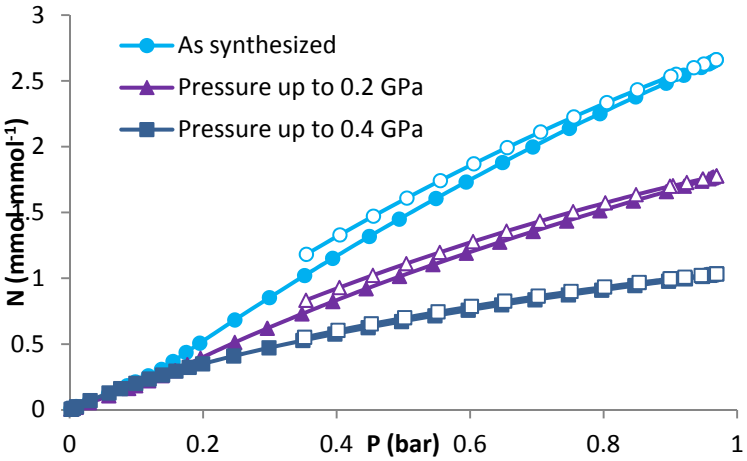

Figure S14. CO_2 adsorption isotherms at 298 K for **1** before and after the mechanical stress tests. Desorption branches of the isotherms are depicted with empty symbols.

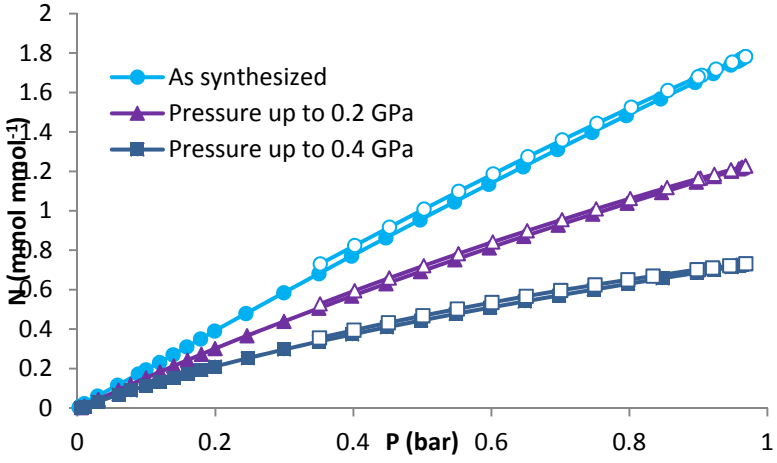

Figure S15 . CO_2 adsorption isotherms at 323 K for **1** before and after the mechanical stress tests. Desorption branches of the isotherms are depicted with empty symbols.

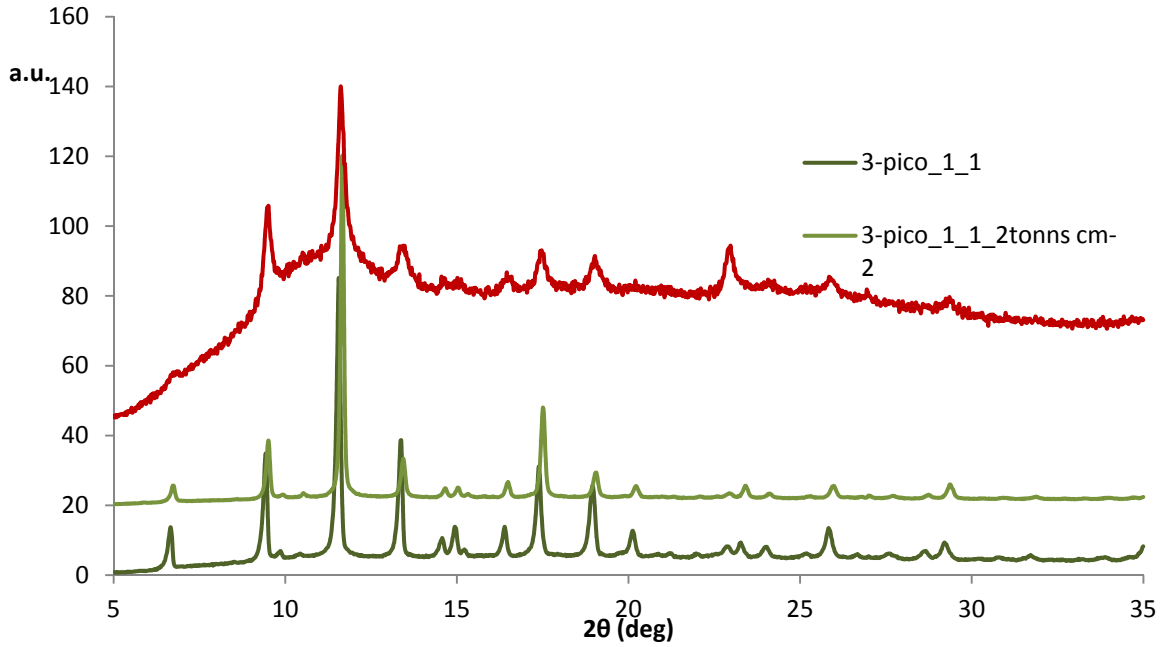

Figure S16. XRPD data for **1@3pico** before and after the mechanical stress tests.

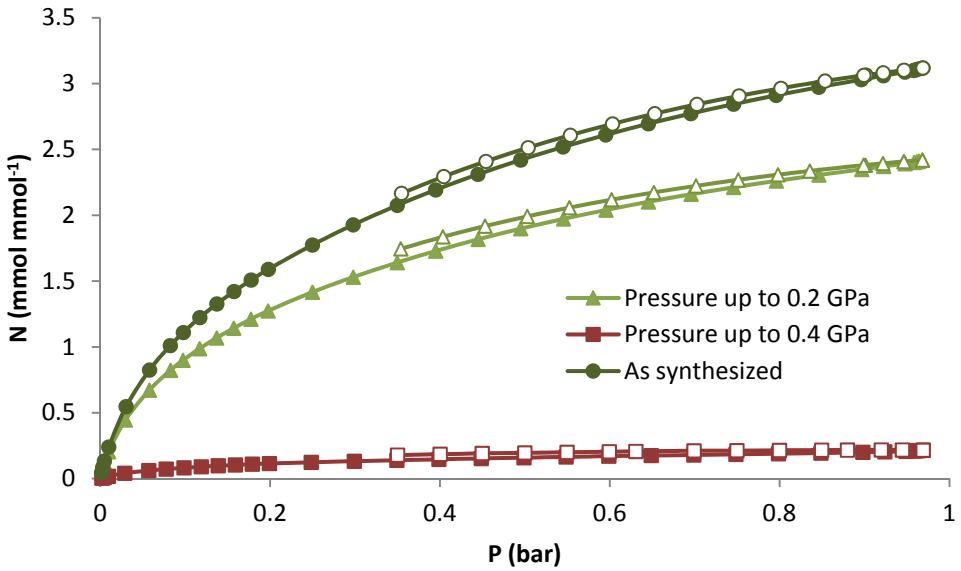

Figure S17. CO_2 adsorption isotherms at 273 K for **1@3pico** before and after the mechanical stress tests. Desorption branches of the isotherms are depicted with empty symbols.

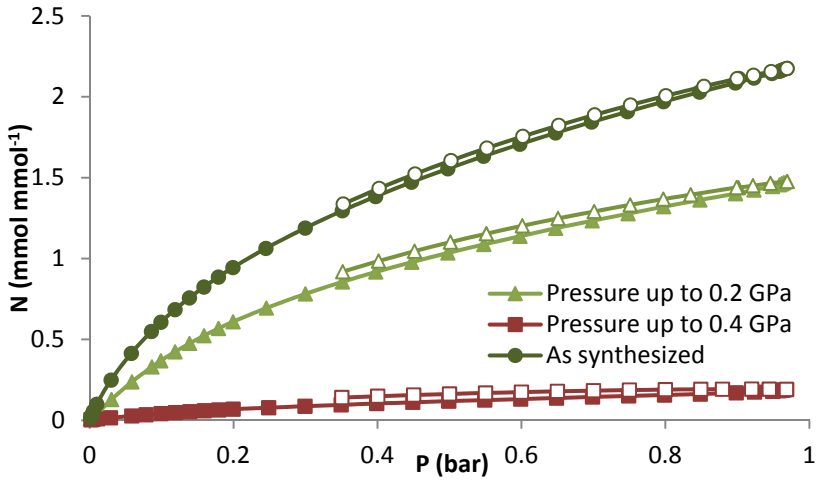

Figure S18. CO_2 adsorption isotherms at 298 K for **1@3pico** before and after the mechanical stress tests. Desorption branches of the isotherms are depicted with empty symbols.

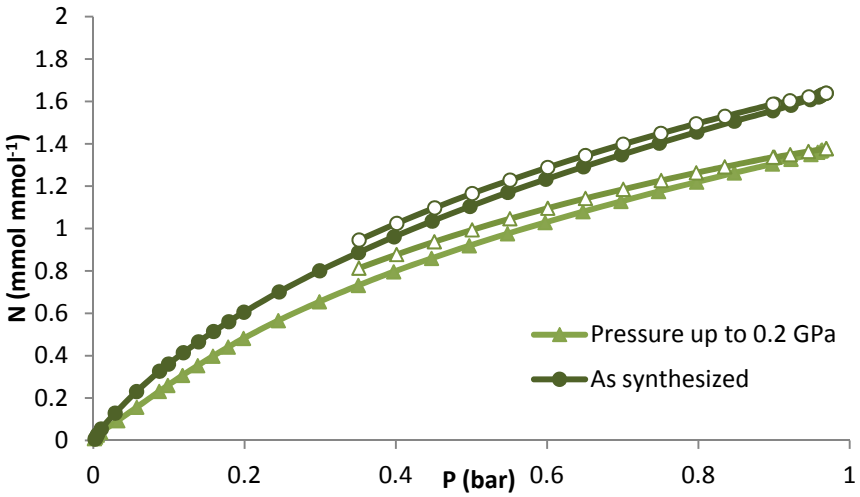

Figure S19. CO_2 adsorption isotherms at 323 K for **1@3pico** before and after the mechanical stress tests. Desorption branches of the isotherms are depicted with empty symbols.

Dynamic Gas Adsorption Experiments

Variable temperature pulse chromatography

Gas-phase adsorption at zero coverage surface was studied using the pulse chromatographic technique employing a Gas Chromatograph and a 15 cm-column (0.4 cm internal diameter) packed with *ca.* 1 g of 0.5 mm-pellets of the studied materials. As the particles of HKUST-1_3pico$_3$ were too small, and in order to avoid column pressure drops, the particles were aggregated by pressuring them up to 0.2 GPa for 1 minute. The resulting pills were grounded trough a 0.5 mm sieve and characterized by XRPD and CO_2 adsorption, showing that there is no loss of crystallinity and porosity. HKUST-1 was treated in a similar way to HKUST-1_3pico$_3$. Prior to measurement, samples were outgassed to 10^{-1} Pa and heated 7 h at 453 K for HKUST-1 and at 393 K for HKUST-1_3pico$_3$. The columns were conditioned in He flow (30 mL min^{-1}). Later on, 2 μL of each gas was injected at 1 bar and the separation performance of the chromatographic column was examined at different temperatures (313 K-333 K).

Breakthrough curves

The gas-separation properties of **1** and **1@3pico** were also examined by breakthrough experiments using dry conditions (1.4 mL min^{-1} CO_2 flux and 8.6 mL min^{-1} N_2 flux) in the 273 -323 K and humid conditions by flowing the gas mixture through a water bath at 323 K. Helium gas was initially purged into the packed column. The relative amounts of the gases passing through the column were monitored on a mass spectrometer gas analysis system (Pfeiffer Vacoon) detecting ion peak at m/z 44 (carbon dioxide), 28 (nitrogen) and 18 (water).

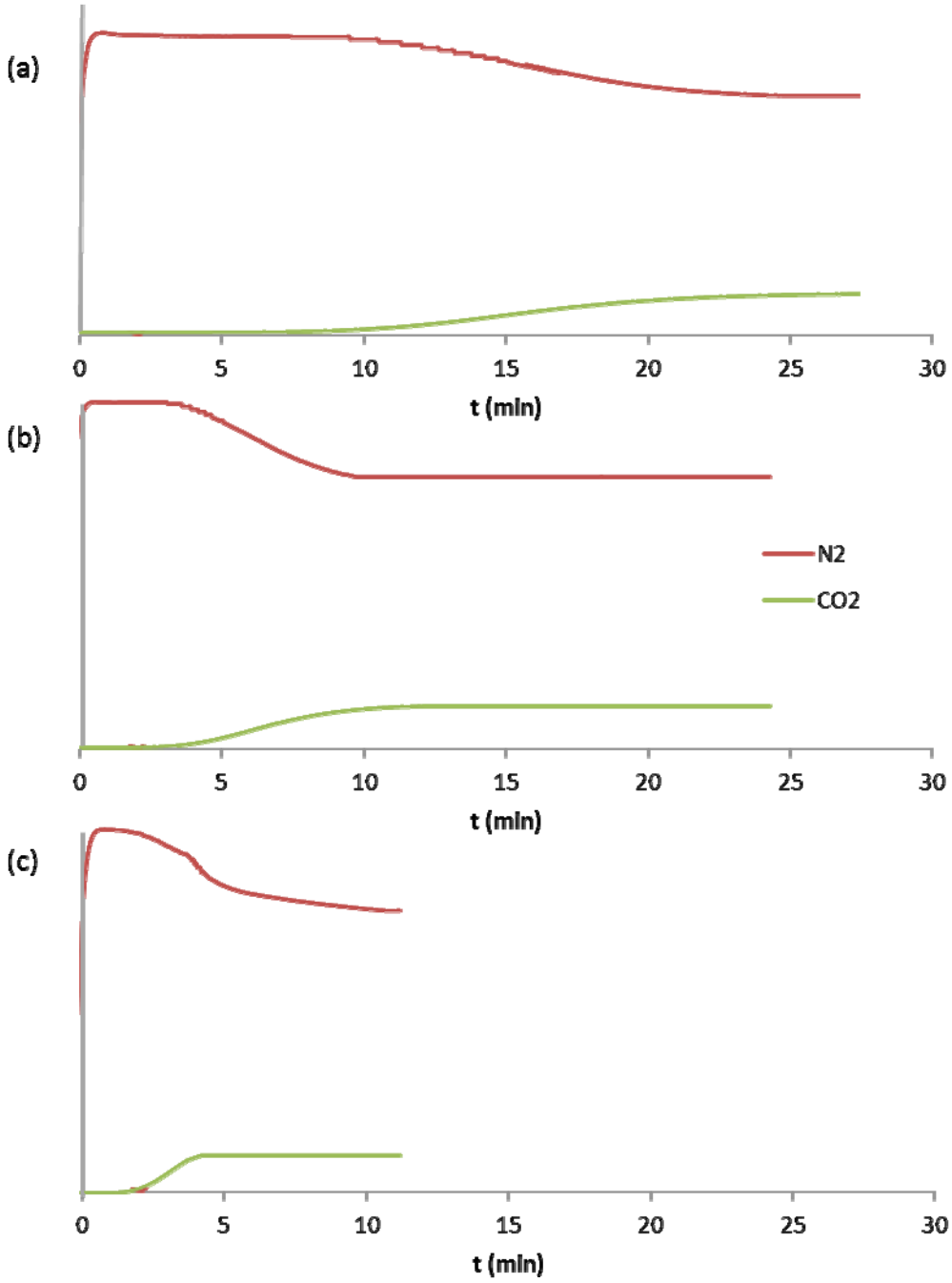

Figure S20. Breakthrough curves of **1** in dry conditions at 273K (a), 298 K (b) and 323 K (c).

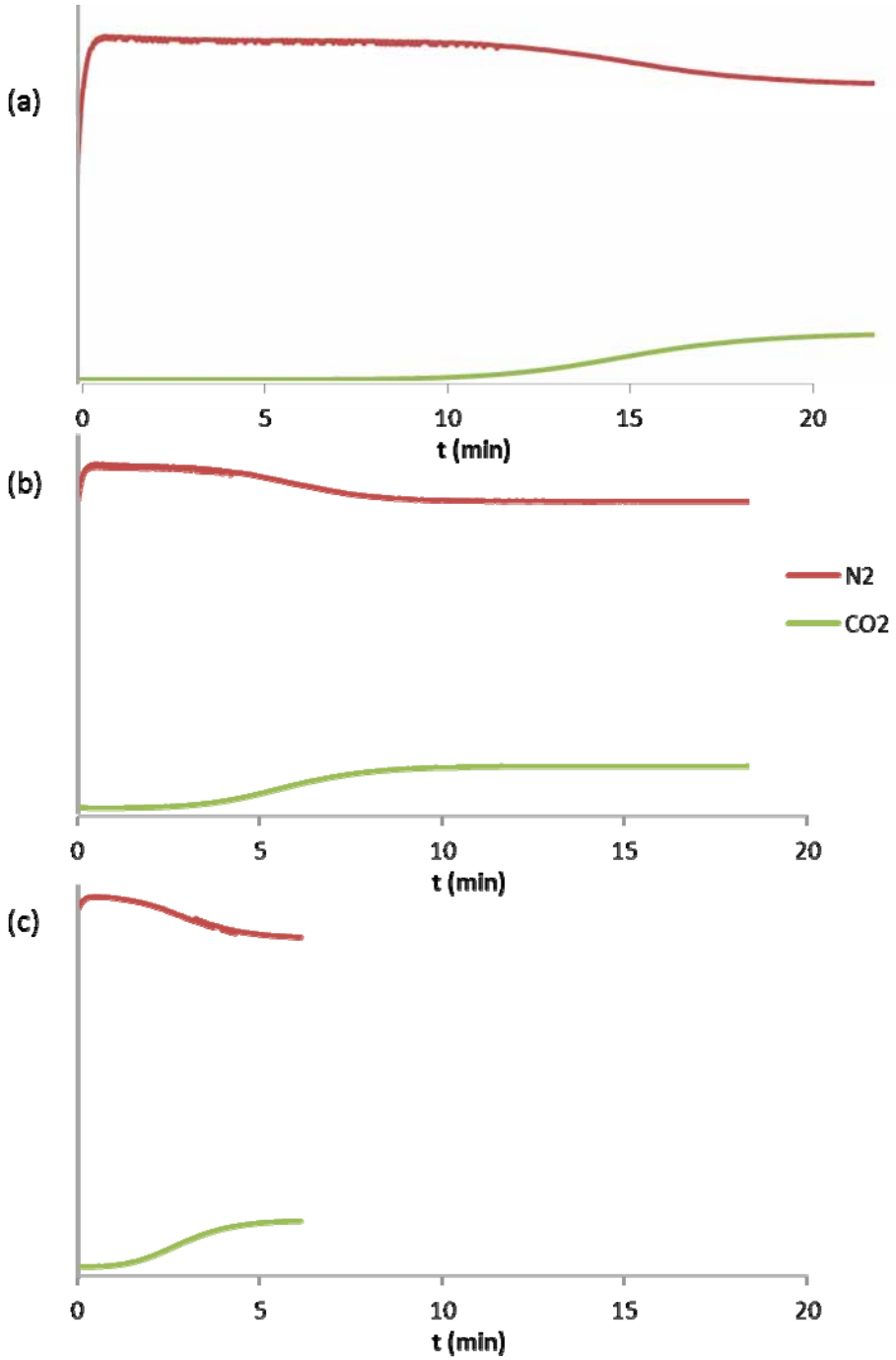

Figure S21. Breakthrough curves of **1@3pico** in dry conditions at 273K (a), 298 K (b) and 323 K (c).

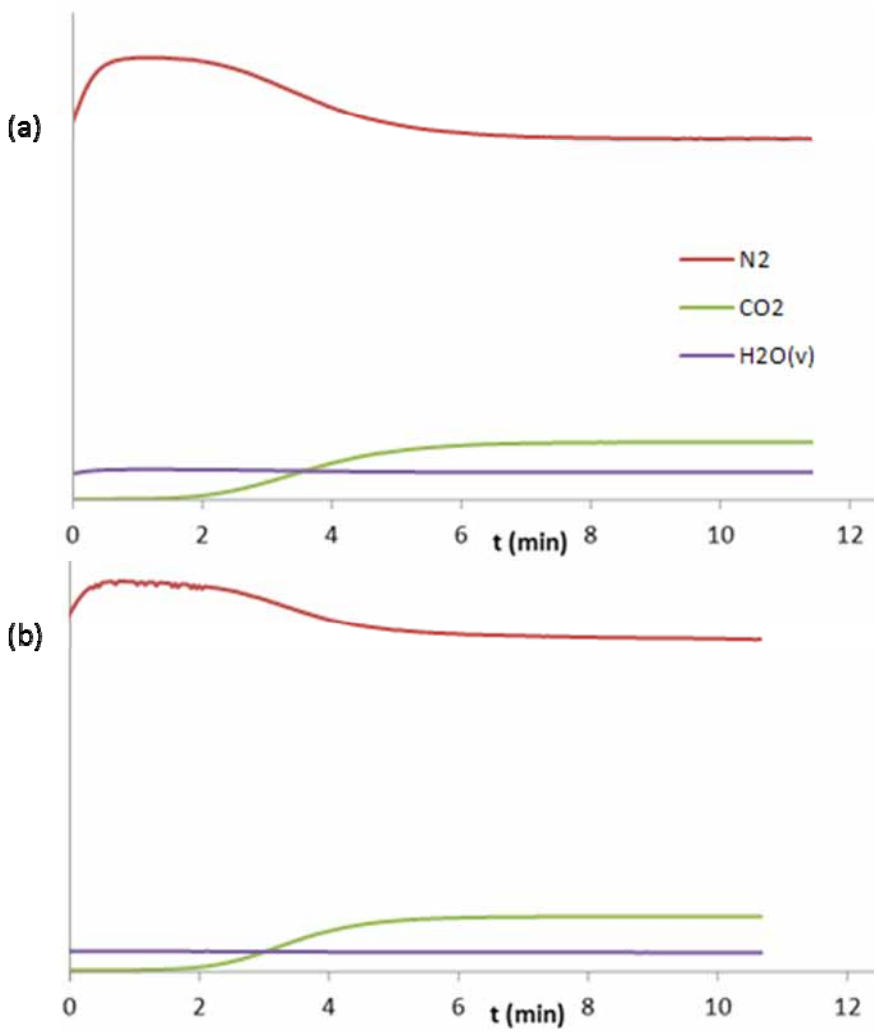

Figure S22. Breakthrough curves of **1**(a) and **1@3pico** (b) in humid conditions at 323K.

Notes and References

[1] K. Schlichte, T. Kratzke, S. Kaskel, *Microporous and mesoporous material*, **2004**, *73*, 81–88.

[2] Y. K. Hwang, D.-Y. Hong, J.-S. Chang, S. H. Jhung, Y.-K. Seo, J. Kim, V. Vimont, M. Daturi, C. Serre, G. Férey, *Angew. Chem., Int. Ed.*, **2008**, *47*, 4144.